J Math Chem (2012) 50:359–373
DOI 10.1007/s10910-010-9772-5

ORIGINAL PAPER

Modelling a P-FAIMS with multiphysics FEM

Raquel Cumeras · Isabel Gràcia · Eduard Figueras · Luis Fonseca · Joaquin Santander · Marc Salleras · Carlos Calaza · Neus Sabaté · Carles Cané

Received: 23 September 2010 / Accepted: 25 October 2010 / Published online: 17 November 2010

Abstract A micro Planar high-Field Asymmetric waveform Ion Mobility Spectrometer (P-FAIMS) operating at ambient pressure and temperature has been simulated using COMSOL Multiphysics software. P-FAIMS is based on ion gas-phase separation due to the dependence of ion mobility with electric field. Ions are selected by a DC voltage characteristic of each ion kind. Physics of ion behaviour in high electric fields conditions is well known but not the chemistry behind ion reactions and kinetics. The aim of this work is the modelling of different kind of ions in a P-FAIMS having account of the main factors involved in their movement in the drift tube. Simulations of vapour phase ions of three compounds have been studied for different values of drift electric field amplitude to gas number density (E/N) ratio: protonated water clusters $H^+(H_2O)_n$ and $O_2^-(H_2O)_n$ ions obtained in air, and a chemical warfare agent simulant $DMMPH^+$ that emulates gas sarin. Ions were selected due to simulation needs of experimental data of the main quantities involved in the definition of ions mobilities. Results show that simulations of ions behaviour in a P-FAIMS are possible with COMSOL Multiphysics software and that the time and intensity at which ions are detected are in good agreement with experimental data from literature.

Keywords FAIMS · FEM gas simulation · Ion mobility spectrometer · COMSOL

This is one of several papers published in Journal of Mathematical Chemistry, "Special Issue: CMMSE 2010", with invited editorial contribution by Prof. Jesus Vigo-Aguiar.

R. Cumeras (✉) · I. Gràcia · E. Figueras · L. Fonseca · J. Santander · M. Salleras · C. Calaza · N. Sabaté · C. Cané
Instituto de Microelectrónica de Barcelona, IMB-CNM (CSIC), Esfera UAB, 08193 Bellaterra, Barcelona, Spain
e-mail: raquel.cumeras@imb-cnm.csic.es

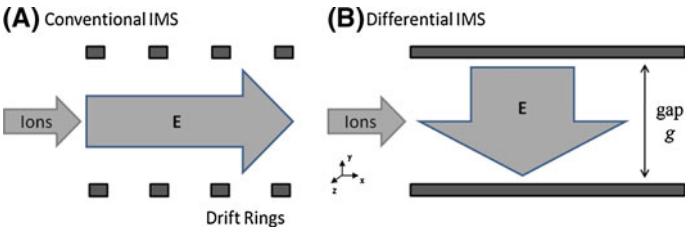

Fig. 1 Diagrams of ions and electric field E application in (**a**) conventional and (**b**) differential IMS

1 Introduction

Ion Mobility Spectrometry (IMS) is an analytical technique based on ion separation in gaseous phase due to an electric field. The science and technology of IMS has been developing rapidly over the last decades and now branches in two subfields: conventional and differential IMS. The fundamental distinction between them is in the physical quantity underlying the separation (the separation parameter):

(1) Conventional IMS includes methods based on the different mobility values of ions and uses electric fields (E) on the same direction that ions displacement (shown in Fig. 1), so that ions entering at the same time are separated according to their mobility reaching the detector at different times [1].
(2) Differential IMS uses an E field perpendicular to ions displacement to separate and select them (shown in Fig. 1). This is allowed taking advantage of the slightly dependence of the ion mobility with strong fields. Using an adequate AC E field the ions are displaced of their main path depending of their mobility dependence to the E field, and only one type can reach the detector [2–4]. Due to the novelty of this technique, it has received multiplicity of names, as is common for emerging technologies, but the prevailing one today is (high) Field Asymmetric waveform IMS (FAIMS), indicating the implementation of a strong time-dependent electric field as a periodic asymmetric waveform.

FAIMS technology uses two main electrodes configurations: cylindrical or planar. In this work we focus on the planar configuration as it is going to be easier to fabricate the device once simulated.

2 Theory

2.1 Ion dynamics

Ions moving in a gas-phase medium and in presence of an electric field E, are accelerated due to coulomb forces and slowed due to collisions with molecules of the gas medium. As a result, the ions move in average at a constant velocity v, proportional to the electric field and in the same direction [5].

The proportional factor is call mobility, K, and usually is expressed in $cm^2/V\,s$:

$$K = v/E \tag{1}$$

And also, ion mobilities depend on E/N, where N is the number density (the number of molecules per unit volume), as it was demonstrated in the earliest studies of ions in gases at the beginning of 20th century [6]. The parameter E/N was introduced due to the need to extend the comparison of results. E/N is expressed in $V\,cm^2$, but for convenience, it was resolved to adopt the unit Townsend: $1\ Td = 10^{-21}\ V\,m^2$ [7,8].

Mobility is usually considered constant in front of E. That can be assumed as true for almost all the practice cases, particularly in the design of conventional IMS. However, for high values of E, K varies.

The mobility (K) and the diffusion coefficient (D) of an ion are connected by the Nernst-Townsend-Einstein relationship [5]:

$$K = \frac{Dq}{k_B T} \tag{2}$$

where q is the ion charge, k_B is the Boltzmann constant, and T is the gas temperature.

A molecule will diffuse differently in different media; hence D is a property of the pair of diffusing and media molecules. For diffusion in gases, D is determined by [5]:

$$D = \frac{3}{16}\left(\frac{2\pi k_B T}{\mu}\right)^{1/2}\frac{1}{N\Omega} \tag{3}$$

where N is the number density (the number of molecules per unit volume), $\mu = mM/(m+M)$ is the reduced mass of the pair of diffusing ion and carrier gas molecule (with respective masses of m and M), and Ω is the collision cross section (the first-order binary collision integral of the pair ion-neutral, from an infinite number of collision integrals defined in the transport theory).

Hence, the mobility of an ion also depends on Ω, according to the theory of Chapman-Enskog, we obtain the Mason-Champ equation:

$$K = \frac{3}{16}\left(\frac{2\pi}{\mu k_B T}\right)^{1/2}\frac{ze}{N\Omega} \tag{4}$$

Equations 2 and 4 apply only for low E/N and need amendments at higher E/N. The mobility of an ion under the effects of high electrical fields can be expressed empirically by [5]:

$$K\left(\frac{E}{N}\right) = K(0)\left[1 + \alpha\left(\frac{E}{N}\right)\right] \tag{5}$$

where $K(0) = K(E)_{|E=0}$ is the mobility of the ion for a low electrical field as defined by Eq. 4. The function $\alpha(E/N)$ takes account of the dependence of the

ion mobility with the electrical field for a constant gas density, at ambient pressure and temperature. The term, $\alpha(E/N)$ can be negative, positive or null for an ion (indifferently of its polarity), and it describes the slope and the direction of the graph of $K(E)$ as a function of E/N [9], as shown in Fig. 2. For physical reasons $K(E/N)$ must be always positive ($K > 0$). That means that in any case alpha must be greater than -1. The experimental data gives values of alpha in the range [−0,01, +0,30].

When the electrical field exceeds the ∼10.000 V/cm (equivalent to 40 Td for $N = 2.687 \times 10^{25}$ m^{-3}) the coefficient of mobility of some ions is increased, reduced or is kept unchanged. At present there is no model that explains correctly the dependence of the coefficient of mobility with the electrical field, there are only certain models of hypotheses that are based in the equation of Mason Schamp (4).

The approximation for the function $\alpha(E/N)$ corresponds to a Taylor's series, where for its definition it has to accomplish that it is equal to 0 for low E, and that it has to have the same value for E than for $-E$, so the terms of odd powers have to be zero,

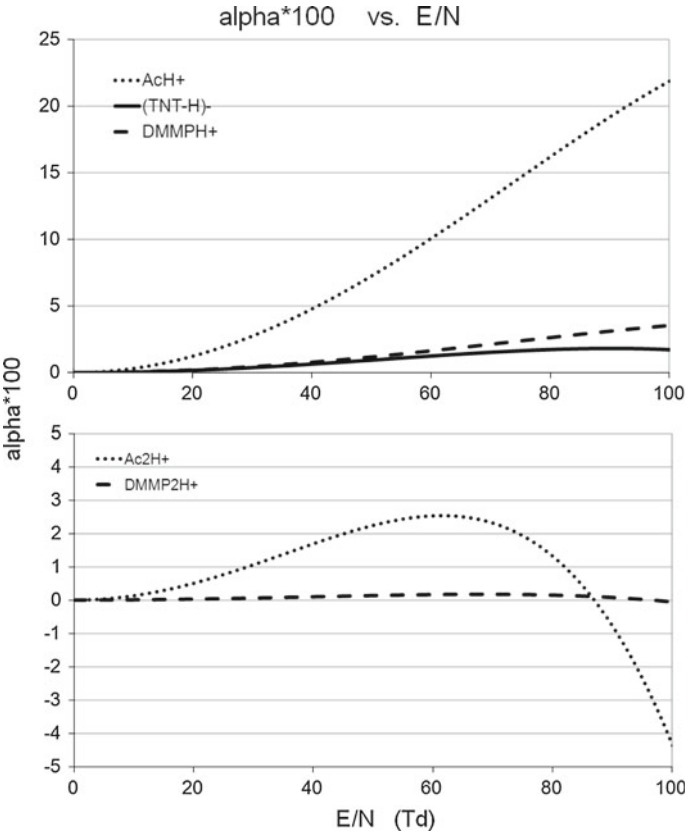

Fig. 2 Plots of alpha parameter related to the electric field drift to gas number density ratio. *Top frame* is for monomers and *bottom frame* is for dimers of some compounds: 2-propanone or acetone (Ac), 2,4,6-trinitrotoluene (TNT) and dimethylmethyl phosphonate (DMMP) that emulates the gas sarin

or almost their sum. $K(E/N)$ expanded into infinite series of powers of E/N, since only even powers may be present:

$$K\left(\frac{E}{N}\right) = K(0)\left(1+\sum_{n=1}^{\infty}\alpha_{2n}\cdot\left(\frac{E}{N}\right)^{2n}\right)$$
$$= K(0)\left[1+\alpha_2\cdot\left(\frac{E}{N}\right)^{2}+\alpha_4\cdot\left(\frac{E}{N}\right)^{4}+\cdots\right] \quad (6)$$

where experimental measurements have shown that α_2 is three to five orders of magnitude smaller than one and α_4 is two orders of magnitude smaller than α_2. So, in practice, with only two factors is enough to calculate the dependence of the mobility with the electric field.

All α_{2n} values may be positive and/or negative depending on the ion-neutral potential Φ among other factors. However, none is null and $\alpha(E/N)$ is never exactly zero, though can be near-zero over a broad range of E/N. The n coefficients could, in principle, be derived [5] from higher-order collision integrals of Ω using elaborated formalisms that will not be reported here.

2.2 Optimum FAIMS separation

In conventional IMS, different species have different v and are separated by the mobility coefficient [5]:

$$v = KE \quad (7)$$

Ions in a fixed E have a constant v and the displacement d is proportional to time:

$$d = KEt \quad (8)$$

For high electric fields in differential IMS, v and d only depends on mobility on y-axe, for x-axe v and d depend only of the drift gas flow, normally air or N_2:

$$v_y(t) = K\left(\frac{E(t)}{N}\right)E(t) = \frac{\partial y}{\partial t} \quad (9)$$

$$\int_{d_0}^{d_y} dy = \int_0^t K\left(\frac{E(t)}{N}\right)E(t)\,dt \quad (10)$$

$$d_y = K(0)\cdot N\times\left[\frac{1}{N}\int_0^t E(t)\,dt+\frac{\alpha_2}{N^3}\int_0^t E^3(t)\,dt+\frac{\alpha_4}{N^5}\int_0^t E^5(t)\,dt\right] \quad (11)$$

The first term of Eq. 11 does not take account of the differences of mobility due to electric field for the different ions and experimentally it is know that α_2 and α_4 are

smaller than 1 [5,10]. So, the only way to take advantage of the dependence of K with E is that the integral of E along t must be zero but not so E^3 and E^5. That implies an asymmetric AC voltage.

Our focus will be on the form of $E(t)$, so it is convenient to normalize [11–13]:

$$E(t) = E_D F(t) \tag{12}$$

where E_D is the amplitude of $E(t)$ also called dispersion field, and $F(t)$ defines the profile.

To measure the difference between K at two values of E, one must send ions on paths where, for a period t_C of the asymmetric AC voltage, the first but not the second or the third term on the right hand side of Eq. 11 cancels. To nullify the first term, $F(t)$ in the range 0 to t_C, must nullify [11–13]:

$$\int_0^{t_C} F(t)\, dt = 0 \tag{13}$$

Equation 13 is trivially met when $F_+(t) = -F_-(t + const)$, an harmonic with t_C period is one example. Formally, at least some odd momenta of $F_+(t)$ and $F_-(t)$ must be unequal [10], i.e.:

$$\langle F_{2n+1} \rangle = \frac{1}{t_C} \int_0^{t_C} F^{2n+1}(t)\, dt \neq 0 \tag{14}$$

for at least one integer $n \geq 1$. The value of n that controls the separation in some regime is the separation order. FAIMS must be viewed as a differential IMS employing primarily $n = 1$ [10,12], while higher-order methods based on $n \geq 2$ were recently conceptualized [11–13]. The quantity $\langle F_{2n+1} \rangle$ characterizing the asymmetry of a particular waveform profile is called the form-factor of order n.

An $F(t)$ that meets Eqs. 13 and 14 comprises two rectangular fragments [14–16]. But this waveform does not consider engineering aspects. An exact rectangular profile cannot be implemented with electrical circuitry. All commercial and most research instruments thus far have used $F(t)$ based on harmonics: bisinuoidal, clipped-sinusoidal forms, etc.

In this work, we focus on bisinusoidal $F(t)$, that is a sinusoidal plus its second overtone phase-shifted by 90°C.

$$F(t) = \frac{1}{f+1}\left[f \sin(wt) + \sin\left(2wt - \frac{\pi}{2}\right)\right] \tag{15}$$

where $w = 2\pi/t_C$ and f is the ratio of amplitudes of first and second harmonics varying from 0 to ∞. Both $f = 0$ and $f = \infty$ converts Eq. 15 to a symmetric sinusoid. Being $f_{opt} = 2$ [3,10]. In Fig. 3 the waveforms generated by Eq. 15 for some values of f are shown.

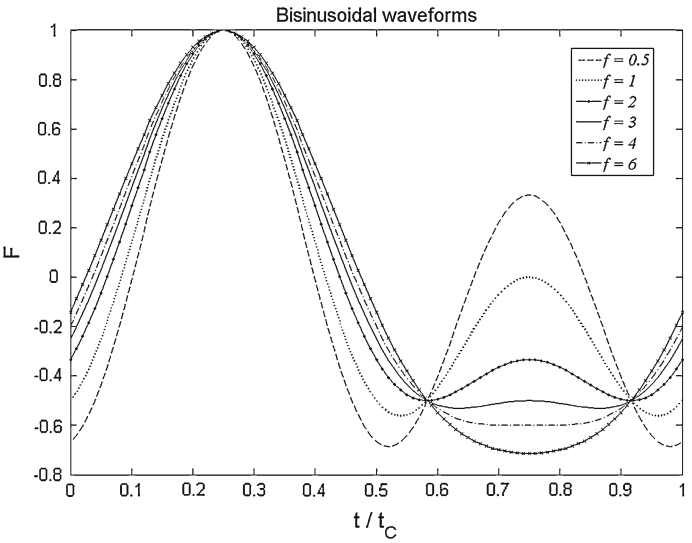

Fig. 3 Bisinusoidal waveforms by Eq. 15 with $f = 0.5, 1, 2, 3, 4$ and 6

2.3 FAIMS filtering using compensation field

The FAIMS filtering is allowed when $\Delta d \ll d_{\max}$, where Δd is the displacement over one oscillation and $d_{\max}$ is the maximum (accumulative) displacement at the end of the FAIMS electrodes. That implies that the gap g between electrodes has to accomplish $\Delta d < g \ll d_{\max}$. If an $E(t)$ is applied between to plates separated by a gap g and ionic species are placed inside, species with $d = 0$ will remain balanced (oscillating around initial positions) whereas the others will drift to one of the boundaries and be destroyed by neutralization. Such device will filter only the ions with $d = 0$, but we can superpose on $E(t)$ a DC voltage or 'compensation voltage' of intensity field E_C that during the period t_C of the asymmetric AC voltage, displaces the ions by:

$$d_C = \int_0^{t_C} K\left[E\left(t\right) + E_C\right] E_C dt \tag{16}$$

For a particular $K(E)$—a particular ion–, one can tune E_C to achieve $d_C = -d$ being the ion is stable in the gap (Fig. 4). The trajectories of ions with unequal $K(E)$ will also change, but the d_C and d values will differ and those ions will still migrate towards their destruction at gap boundaries. Hence, in principle, any species can be uniquely selected using a proper E_C value, and a scanning on E_C would produce the spectrum of present species.

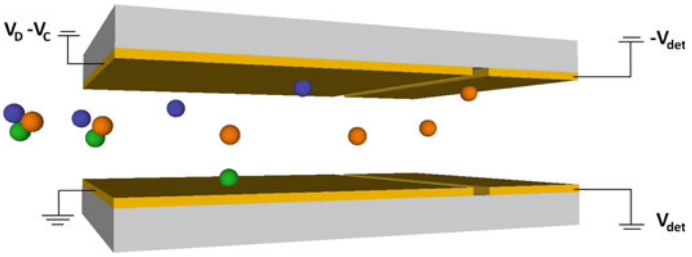

Fig. 4 Schematic of a drift channel defined by P-FAIMS and detector electrodes. Ion paths are schematized under the influence of AC (V_D) and DC (V_C) fields for the filtering region and the detector fields for detection region

2.4 Experimental data

The absolute mobility scale enabling comparisons between IMS data at different N is established by introducing the reduced mobility:

$$K_0 = K\frac{P}{P_0}\frac{T_0}{T} = K\frac{N}{N_0} \tag{17}$$

where the mobility is normalized to pressure P and temperature T for the value for standard conditions for temperature and pressure (STP): $T_0 = 298$ K and $P_0 = 760$ Torr; or to the gas number density (the number of molecules per unit volume), for the value of the Loschmidt constant: $N_0 = 2.687 \times 10^{25}\,\mathrm{m}^{-3}$.

Simulations have been done with experimental data available at the literature [12,17], and the main properties needed: $K(0)$, α_2 and α_4, are summarized in Table 1.

3 Two dimensional modelling for Planar-FAIMS

3.1 Model definition

COMSOL Multiphysics software is used to simulate the behaviour of three different compound ions in a P-FAIMS. The software takes into account nonlinear combined effects of different forces and concentration gradients. Created model combines fluid dynamics and electric field which have been found to be the most significant effects. Other effects such as electric repulsion in ion cloud due to space

Table 1 Parameters used in simulations for studied compounds [12,17]

Chemical	Ion acronym	$K(0)$ $\left(10^{-4}\mathrm{m}^2\,\mathrm{V}^{-1}\,\mathrm{s}^{-1}\right)$	$\alpha_2\left(\mathrm{Td}^{-2}\right)$	$\alpha_4\left(\mathrm{Td}^{-4}\right)$
Positive reactant ion	$H^+(H_2O)$	2.34	1.78×10^{-5}	-4.91×10^{-10}
Negative reactant ion	$O_2^-(H_2O)$	2.13	1.93×10^{-5}	-4.30×10^{-10}
Dimethyl methylphosphonate	$DMMPH^+$	1.94	5.09×10^{-6}	-1.58×10^{-10}

charge have been found to be considerably less significant (for the low concentration level simulated, 1ppm) and thus were not included in the simulations presented [18].

Model assumptions are summarized in Fig. 5. Drift gas velocity in the P-FAIMS gap has been calculated using the Navier-Stokes module for air. Electric potentials applied to the P-FAIMS and detector electrodes are calculated using the conductive media DC module and, the movement of ions are calculated with electrokinetic flow module, which takes into account of ions behaviour.

A 2D approximation of Fig. 4 is done considering that all the effects do not vary along the electrodes width l. Simulations are done considering two electrode regions as shown in Fig. 4: (1) P-FAIMS or *filtering electrodes* where the AC and DC voltages needed to filter the different ionic species are applied, of $13 \times 5\,\text{mm}^2$ separated by 0.5 mm gap, (2) *detector electrodes* (charge collectors) of $5 \times 5\,\text{mm}^2$ that are placed 1 mm after P-FAIMS electrodes to collect ions and generate the V_C spectrum. Drift gas and ions enter the P-FAIMS from the left, passes through the P-FAIMS electrodes and only 'selected' ions reach the detector electrodes. Ions are introduced from the centre of the channel high at the beginning of the P-FAIMS electrodes with a spatial distribution specified as $\Delta y = 0.02$ mm, while air gas flows over all the channel height.

3.2 Electric fields

Detector electrodes have been biased at $\pm$ 5V and total electric voltage applied at the P-FAIMS electrodes has been defined as: $V_T = V_D - V_C$. Applied dispersion voltage V_D accomplish Eq. 15 with $f = 2$ [10]:

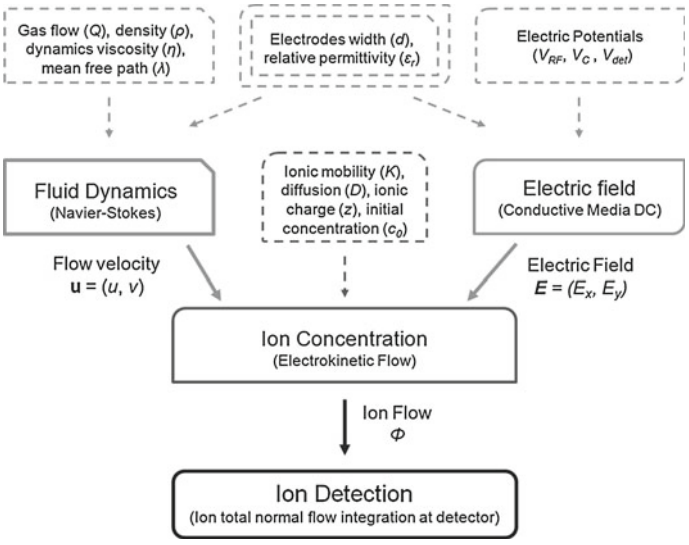

Fig. 5 Block diagram of key computational steps involved in modelling P-FAIMS with COMSOL Multiphysics software. *Straight squares* indicate main modules and *dashed squares* indicate variables needed for the modules

$$V_D(t) = \frac{V_{iD}}{3}\left[2\sin(wt) + \sin\left(2wt - \frac{\pi}{2}\right)\right] \tag{18}$$

where for all simulations, the frequency of the waveform applied has been set to $\nu_{RF} = 2$ MHz [1–3], and is shown in Fig. 6.

It is needed to achieve a compromise between frequency and gap. A low frequency implies that the positive high-voltage V_{max} is applied for a longer time and ions will travel a longer distance toward the P-FAIMS electrodes and eventually they will be lost before reaching the detector.

3.3 Fluid dynamics

Air flow modelling is determined by the incompressible Navier-Stokes equations. Even though a detailed analysis of fluid flow can be extremely difficult, the basic concepts involved in fluid flow problems are fairly straightforward. These basic concepts can be applied in solving fluid flow problems through the use of simplifying assumptions and average values, where appropriate.

To solve Navier-Stokes module, COMSOL software uses the equations:

$$\rho\frac{\partial \mathbf{u}}{\partial t} - \nabla\cdot\eta\left(\nabla\mathbf{u} + (\nabla\mathbf{u})^T\right) + \rho\mathbf{u}\cdot\nabla\mathbf{u} + \nabla p = \mathbf{F} \tag{19}$$

where ρ is the fluid density, $\mathbf{u}$ is the velocity vector, η is the dynamic viscosity, T is the temperature, p is the pressure and $\mathbf{F}$ is the term of forces actuating on the body.

Gas flow in pipes or between parallel plates is in a either laminar or turbulent regime and is determined by the dimensionless Reynolds number. In our case, for an inlet gas flow of $Q = 1$ l/min, Reynolds number obtained is Re ~ 400, this value is 10 times

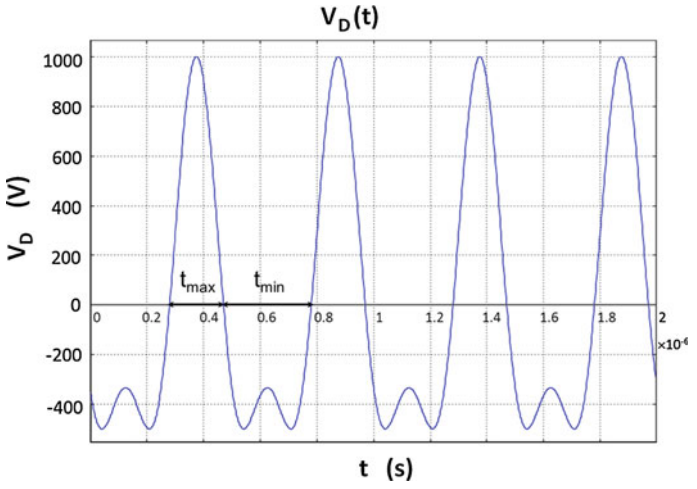

Fig. 6 Dispersion voltage as applied to the modelled P-FAIMS with COMSOL Multiphysics software

lower than the turbulence onset threshold (Re $\sim$ 4.000), so the gas flow is considered to be laminar.

Air simulations have been operated at a temperature of 298 K and a pressure of 760 Torr and number density of air is $N = 2.5 \times 10^{25}\mathrm{m}^{-3}$, and considering that the pressure of air and the ions is the same, so air do not vary its pressure as it is confined between two parallel plates and because the sample enters for the centre of the gap and has no expansion due to the pressure.

3.4 Ion concentration

Flow of charged ions subject to an electric field verifies the mass conservation law defined from Nernst-Planck equation that takes into account diffusion, convection and migration flows:

$$\nabla \cdot (-D\nabla c + \mathbf{u}c - z_{ion} K c \nabla V) = R = 0 \tag{20}$$

where D is ion diffusion $\left(\mathrm{m}^2/\mathrm{s}\right)$, c is ion concentration $\left(\mathrm{mol/m}^3\right)$, z_{ion} is ions charge number (adim.), K is ion mobility coefficient $\left(\mathrm{cm}^2/\mathrm{V\,s}\right)$, V (V) is the voltage affecting the ion, R $\left(\mathrm{mol}/\left(\mathrm{m}^3\,\mathrm{s}\right)\right)$ is reaction rate that is supposed to be zero-Ions do not interact with one another- and $\mathbf{u}$ is the air velocity (m/s) affecting ion species. Previous equation is mass conservation for the total flow of the ionic specie, the electrokinetic flow: $\nabla \cdot (\Phi_{EK}) = 0$, where $\Phi_{EK} = \Phi_D + \Phi_C + \Phi_M$ is the electrokinetic flow and is the sum of: (1) diffusion flow expressed by Fick's law: $\Phi_D = -D\nabla c$ that takes account of ion random movements; (2) convection flow: $\Phi_C = \mathbf{u}c$ that takes account of gas drift velocity; (3) migration flow: $\Phi_M = -z_{ion} K c \nabla V$ that takes account of flow variations due to applied voltages. Concentrations of ions modelled have been fixed to 1 ppm in all studied cases.

3.5 Ion detection

The local concentration of ions within the drift region and its dependence from the parameters above mentioned allows computing the ion current at the collector. Integrating the normal component of ions flux per unit area A $\left(\mathrm{mm}^2\right)$ of the collector with normal vector $\mathbf{n}$ yields the ion current [19]:

$$I = \int_A \mathbf{n} F z_{ion} \boldsymbol{\Phi}_{EK} dA = \int_{x,z} \mathbf{n} F z_{ion} \boldsymbol{\Phi}_{EK} dx dz \overset{2D\ aprox}{=} d \int_x F z_{ion} \boldsymbol{\Phi}_{EK} dx \tag{21}$$

where F (= 96.485 C/mol) is the Faraday constant [20]. As considering 2D simulations we are assuming that z-intensity is uniform for the whole detectors width. This integral has been defined by 'integration coupling variables' option from the COMSOL software, before performing the simulations.

3.6 Simulation simplifications

Modelled ions are analyzed once inside the P-FAIMS, and non-ionized molecules form part of the drift gas. To simplify numerical simulations, following assumptions are made: (1) All ions are singly charged; (2) Ions are assumed to be free from clusters -from water vapour and nitrogen in the ionization process-; (3) Ions do not interact with one another, so that interactions resulting from space charging do not occur; (4) Ions do not have dipolar moment.

4 Results and discussion

The modelled ions correspond to vapour phase compounds of protonated water clusters $H^+(H_2O)_n$ and $O_2^-(H_2O)_n$ ions obtained in air, and a chemical warfare agent simulant positive ion monomer: $DMMPH^+$ that emulates gas sarin. Ions modelled are listed in Table 1 and have been selected because the parameters K_0, α_2 and α_4 that define their movement in high electric fields are available in the literature [12].

In Fig. 7 the modelled velocity field in the drift channel is shown in grey scale and the graphic of the x-velocity of air for an arbitrary x-scale, is superimposed. It can be seen the laminar behaviour of the drift gas flow for an inlet gas flow of $Q = 1$ l/min, with a maximum x-velocity of 10 m/s.

For low RF electric fields ($E/N < 40$ Td, equivalent to an electric field of 10.000 V/cm in air at ambient pressure and temperature) there is no dependence of mobility with electric field, therefore $V_C = 0$ V for all ions. Increasing electric field they can be separated due to their differences on mobility coefficients.

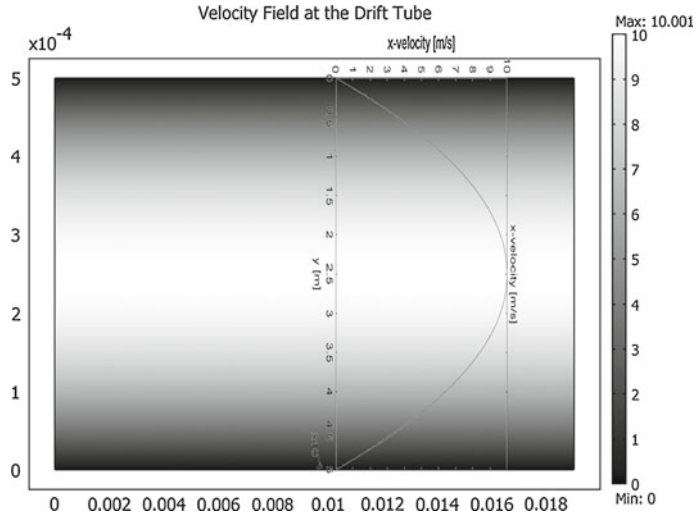

Fig. 7 Velocity field of air at the drift channel obtained with Navier-Stokes module for an inlet gas flow of $Q = 1$ l/min. Superimposed is shown the laminar behaviour of x-velocity of air in an arbitrary x

In Fig. 8, the results for the simulated compounds in air are showed. For $E/N < 40$ Td, is not possible to differentiate the ions and all are detected at the same time, but from $E/N \geq 40$ Td, $DMMPH^+$ ions are differentiated from reactant ions; and for $E/N \geq 70$ Td, also reactant ions $H^+(H_2O)$ and $O_2^-(H_2O)$ are differentiated. What is really interesting is that one can separate accurately a mixture of ionic species just scanning the compensation voltage.

An example of obtained intensity for the different ionic species simulated is shown in Fig. 9 for a $E/N = 70$ Td. Showing that with the proper selection of the applied compensation voltage V_C it is possible to obtain a good separation. Obtained intensities are in the range of experimental ones [11,13]. One has to have really clear that these results have been done for a drift gas of air. If the drift gas is different, obtained compensation voltages will differ from those reported here.

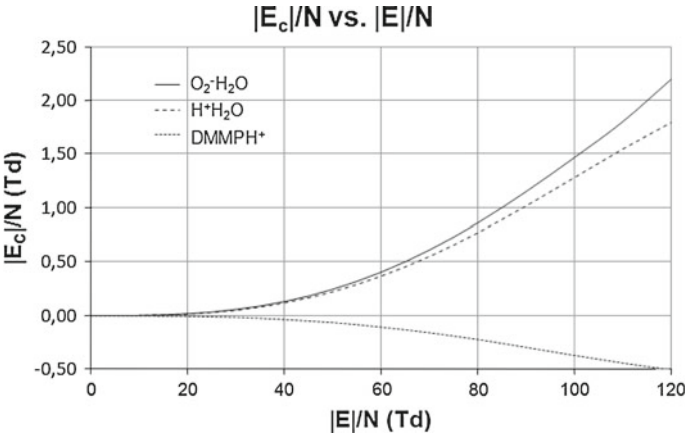

Fig. 8 Obtained compensation fields for simulated compounds

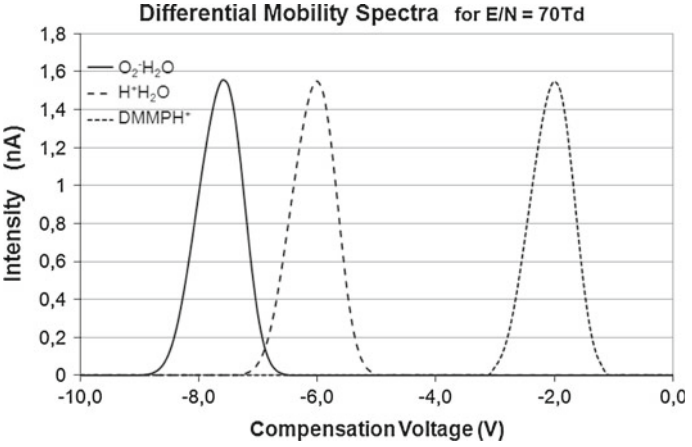

Fig. 9 Obtained intensities for a separation field of $E/N = 70$ Td for simulated compounds. Differentiation is achieved

In Fig. 10, concentrations of the $H^+(H_2O)$ and DMMPH+ ions are presented for an $E/N = 60$ Td. As could be seen in this case of DMMPH+, ion reach the detector for a $V_C = -1.35$ V. For the same compensation voltage, the positive reactant ion peak $H^+(H_2O)$ ion dose not reach the detector. For this E/N the positive reactant ion $H^+(H_2O)$ is detected for $V_C = -4.6$ V, and the negative reactant ion $O_2^-(H_2O)$ is detected for $V_C = -5.5$ V. Therefore, differentiation is also obtained for the three compounds studied.

Results obtained from simulations showed that ion detection could be achieved with COMSOL software and that it is a good platform for this kind of simulations.

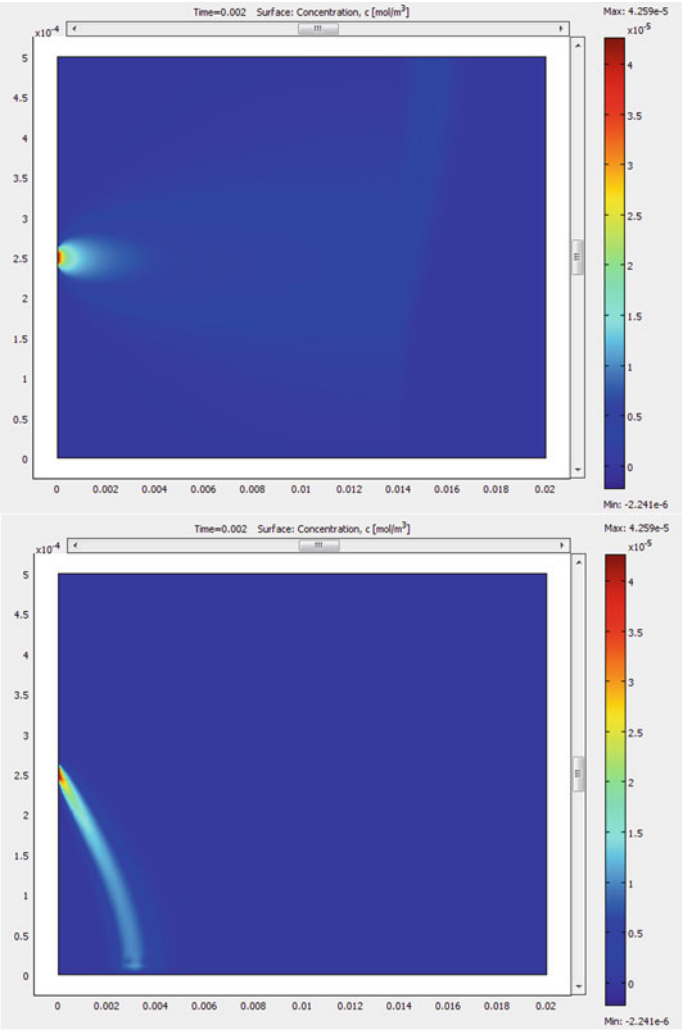

Fig. 10 Concentrations for a separation field of $E/N = 60$ Td, of TOP) $DMMPH^+$ ions and BOTTOM) $H^+(H_2O)_n$ ions; showing that for the same $V_C = -1, 35$ V only the $DMMPH^+$ ion reaches the detector electrode. Differentiation is achieved

Obtained intensities for initial concentrations of 1ppm, are in all cases of the order of nA in accord with experimental ones. For concentrations of 1ppb is expected to obtain intensities of the order of pA.

5 Conclusions and prospect

Simulations of a P-FAIMS have been done with COMSOL Multiphysics software for three compounds in vapour phase. Values of E/N have been studied from 0 to 120 Td, showing that for $E/N < 40$ Td, is not possible to differentiate the ions, in good agreement with experimental data. And from $E/N \geq 40$ Td it is possible to differentiate $DMMPH^+$ ion from reactant ions, and that for $E/N \geq 70$ Td also reactant ions $H^+(H_2O)$ and $O_2^-(H_2O)$ are differentiated.

Acknowledgments This work and Thesis grant of Ms. R. Cumeras have been financially supported by the Spanish Ministry of Science and Innovation MICINN-TEC2007-67962-C04-01 project.

References

1. G.A. Eiceman, Z. Karpas, *Ion Mobility Spectrometry* (CRC Press, Boca Raton, 1993)
2. R.A. Miller, G.A. Eiceman, E.G. Nazarov, A.T. King, Sens. Actuator B-Chem. **67**, 300–306 (2000)
3. R. Guevremont, R.W. Purves, Rev. Sci. Instrum. **70**, 1370–1383 (1999)
4. M. Salleras, A. Kalms, A. Krenkow, M. Kessler, J. Goebel, G. Muller, S. Marco, Sens. Actuator B-Chem. **118**, 338–342 (2006)
5. E.A. Mason, E.W. McDaniel, *Transport Properties of Ions in Gases* (Wiley, New York, 1988)
6. J.J. Thomson, G.P. Thomson, *Conduction of Electricity Through Gases* (University Press, Cambridge, 1928)
7. L.G.H. Huxley, R.W. Crompton, M.T. Elford, Br. J. Appl. Phys. **17**, 1237–1238 (1966)
8. The Editor, Br. J. Appl. Phys. **18**, 691 (1967)
9. G.A. Eiceman, B. Tadjikov, E. Krylov, E.G. Nazarov, R.A. Miller, J. Westbrook, P. Funk, J. Chromatogr. A **917**, 205–217 (2001)
10. A.A. Shvartsburg, *Differential Ion Mobility Spectrometry: Nonlinear Ion Transport and Fundamentals of FAIMS* (CRC Press, Boca Raton, FL, 2009)
11. E.V. Krylov, Int. J. Mass Spectrom. **225**, 39–51 (2003)
12. E.V. Krylov, E.G. Nazarov, R.A. Miller, Int. J. Mass Spectrom. **266**, 76–85 (2007)
13. I.A. Buryakov, Talanta **61**, 369–375 (2003)
14. E.V. Krylov, Technol. Phys. **44**, 113–116 (1999)
15. E.V. Krylov, Instrum. Exp. Tech. **40**, 628–631 (1997)
16. D. Papanastasiou, H. Wollnik, G. Rico, F. Tadjimukhamedov, W. Mueller, G.A. Eiceman, J. Phys. Chem. A **112**, 3638–3645 (2008)
17. N. Krylova, E. Krylov, G.A. Eiceman, J.A. Stone, J. Phys. Chem. A **107**, 3648–3654 (2003)
18. D.A. Dahl, T.R. McJunkin, J.R. Scott, Int. J. Mass Spectrom. **266**, 156–165 (2007)
19. S. Barth, W. Baether, S. Zimmermann, Sens. J. IEEE **9**, 377–382 (2009)
20. NIST. Chemistry WebBook. Available from: http://webbook.nist.gov/chemistry